



## **Intravitreal bevacizumab upregulates transthyretin in experimental branch retinal vein occlusion**

Cehofski, Lasse Jørgensen; Kruse, Anders; Alsing, Alexander Nørgard; Nielsen, Jonas Ellegaard; Pedersen, Shona; Kirkeby, Svend; Honoré, Bent; Vorum, Henrik

*Published in:*  
Molecular Vision

*Publication date:*  
2018

*Document version*  
Publisher's PDF, also known as Version of record

*Citation for published version (APA):*  
Cehofski, L. J., Kruse, A., Alsing, A. N., Nielsen, J. E., Pedersen, S., Kirkeby, S., Honoré, B., & Vorum, H. (2018). Intravitreal bevacizumab upregulates transthyretin in experimental branch retinal vein occlusion. *Molecular Vision*, 24, 759-766.

# Intravitreal bevacizumab upregulates transthyretin in experimental branch retinal vein occlusion

Lasse Jørgensen Cehofski,<sup>1,2,3</sup> Anders Kruse,<sup>1</sup> Alexander Nørgård Alsing,<sup>1,2,3</sup> Jonas Ellegaard Nielsen,<sup>4</sup> Shona Pedersen,<sup>3,4</sup> Svend Kirkeby,<sup>5</sup> Bent Honoré,<sup>3,6</sup> Henrik Vorum<sup>1,3</sup>

<sup>1</sup>Department of Ophthalmology, Aalborg University Hospital, Aalborg, Denmark; <sup>2</sup>Biomedical Research Laboratory, Aalborg University Hospital, Aalborg, Denmark; <sup>3</sup>Department of Clinical Medicine, Aalborg University, Aalborg, Denmark; <sup>4</sup>Department of Clinical Biochemistry, Aalborg University Hospital, Aalborg, Denmark; <sup>5</sup>Department of Odontology, School of Dentistry, University of Copenhagen, Copenhagen, Denmark; <sup>6</sup>Department of Biomedicine, Aarhus University, Aarhus, Denmark

**Purpose:** To identify retinal protein changes that mediate beneficial effects of intravitreal bevacizumab in experimental branch retinal vein occlusion (BRVO).

**Methods:** In six Danish Landrace pigs, BRVO was induced with argon laser in both eyes. After BRVO was induced, the right eye of each animal was given an intravitreal injection of bevacizumab while the left eye was treated with saline water. The retinas were collected 15 days after BRVO, and differentially expressed proteins were analyzed with tandem mass tags–based mass spectrometry. Validation of statistically significantly changed proteins was performed with immunohistochemistry and western blotting.

**Results:** Fluorescein angiography showed no recanalization of the occluded vessels. A total of 4,013 proteins were successfully identified and quantified. Nine proteins were statistically significantly changed following bevacizumab intervention. In experimental BRVO, bevacizumab treatment resulted in upregulation of transthyretin (TTR) and pan-tothenate kinase 3. Bevacizumab downregulated protocadherin 7, protein FAM192A, and ATP synthase protein 8. Immunohistochemistry revealed that TTR was highly abundant in the choroid following bevacizumab intervention.

**Conclusions:** Bevacizumab intervention in experimental BRVO resulted in an increased level of TTR. This is the second study in which we showed an increased retinal level of TTR following anti-vascular endothelial growth factor (VEGF) intervention in experimental BRVO. We hypothesize that there is an interaction between TTR and VEGF and that bevacizumab may exert a beneficial effect on the retina by upregulating TTR.

Branch retinal vein occlusion (BRVO) is one of the most common retinal vascular diseases [1]. Loss of visual function in BRVO is often caused by macular edema. Bevacizumab is an anti-vascular endothelial growth factor (VEGF) agent frequently used for the treatment of macular edema following BRVO. Bevacizumab is a full-length monoclonal immunoglobulin G (IgG) antibody that binds and neutralizes all isoforms of VEGF-A [2]. Although the efficacy of bevacizumab is well documented, there is only limited knowledge about the large-scale retinal protein changes caused by bevacizumab in BRVO [3].

Inhibition of VEGF with bevacizumab is likely to change the retinal content of a multitude of proteins. Proteins that mediate the beneficial effect of bevacizumab may serve as potential therapeutic targets and may be useful in improving existing anti-VEGF regimens. In the present study, an intravitreal bevacizumab intervention was tested in an

experimental porcine model of BRVO followed by proteomics analysis.

## METHODS

**Animal preparation:** The study was approved by the Danish Animal Experiments Inspectorate, permission no. 2016–0201-00971, and the experiments were conducted in accordance with the guidelines published by the Institute for Laboratory Animal Research. The study was conducted in adherence to the ARVO Statement for the Use of Animals in Ophthalmic and Vision Research. The animals were housed under a 12 h:12 h light-dark cycle. Anesthesia was performed with an intramuscular injection of Zoletil mixture consisting of ketamine 6.25 mg/ml and tiletamine 6.25 mg/ml, zolazepam 6.25 mg/ml, butorphanol 1.25 mg/ml, and xylazine 6.5 mg/ml. The dosage of the Zoletil mixture was 1 ml/10 kg. Dilatation of the pupils was performed as described in a previous work [4].

**Branch retinal vein occlusion and bevacizumab intervention:** An experimental overview is provided in Figure 1. Six Danish Landrace pigs were used for the experiments. BRVO was induced in both eyes of the animals by occluding

Correspondence to: Lasse Jørgensen Cehofski, Department of Ophthalmology, Aalborg University Hospital, Hobrovej 18-22, 9000 Aalborg, Denmark; Phone +45 53558878; FAX:+45 97662581; email: [lassecehofski@hotmail.com](mailto:lassecehofski@hotmail.com)

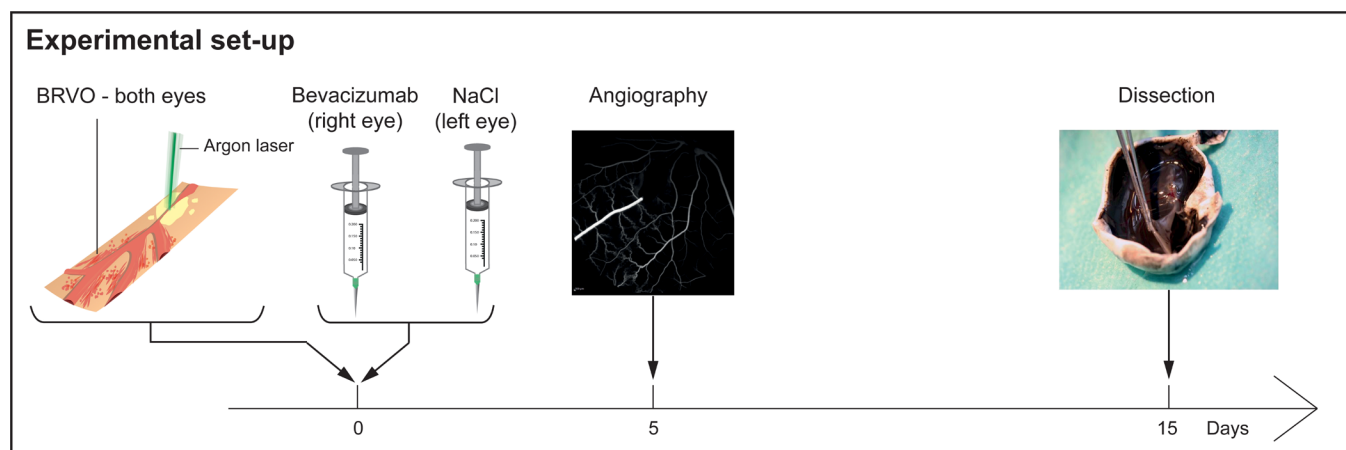


Figure 1. Experimental overview. Branch retinal vein occlusion (BRVO) was induced in both eyes of six Danish Landrace pigs. After successful occlusion had been observed, the right eyes were given an intervention with bevacizumab while the left eyes received an injection containing saline water (NaCl). Fluorescein angiography was conducted 5 days after BRVO to confirm that the veins remained occluded. The eyes were enucleated and dissected 15 days after BRVO. Paired retinal samples from five animals were used for proteomic analysis with mass spectrometry followed by western blotting. Thus, samples with BRVO + bevacizumab (n=5) were compared to BRVO + NaCl (n=5). Eyes from one animal were used for validation with immunohistochemistry.

a branch retinal vein in the inferior retina as described in previous works [4,5]. Briefly, BRVO was induced close to the optic head with a standard argon laser (532 nm) given by indirect ophthalmoscopy using a 20 D lens. The laser settings were 400 mW and 550 ms. A total of 30–40 laser applications were used per occlusion. BRVO was considered successful when flame-shaped hemorrhages appeared and stagnation of venous blood was observed.

Before the intravitreal injections, povidone iodine eye drops were applied in both eyes (Skanderborg Pharmacy, Skanderborg, Denmark). Approximately 15 min after successful BRVO was observed, the right eyes received an intravitreal injection of 0.05 ml bevacizumab 25 mg/ml (Avastin, Roche, Hvidovre, Denmark). The left eyes were given an intravitreal injection of 0.05 ml sodium chloride 9 mg/ml (NaCl; B. Braun, Frederiksberg, Denmark). After the injections, chloramphenicol ointment 1% (Takeda Pharma A/S, Taastrup, Denmark) was applied in both eyes. Fluorescein angiography was performed 5 days after BRVO to confirm that the veins remained occluded. Fifteen days after BRVO, the eyes were enucleated, and the animals were euthanized immediately after enucleation. Euthanasia was performed with an intravenous injection of Euthasol (Virbac Danmark A/S, Kolding, Denmark) 400 mg/ml, 0.5 ml/kg.

**Sample preparation for mass spectrometry:** Right eyes (bevacizumab, n=5) and left eyes (NaCl, n=5) from five animals were used for mass spectrometry based on quantification with tandem mass tags (TMT). The neurosensory retinas were collected as previously described [4] and stored at  $-80^{\circ}\text{C}$

until further use. One hundred micrograms from each of the ten retinal samples were transferred to a new tube, and 100 mM triethyl ammonium bicarbonate (TEAB) were added until a volume of 100  $\mu\text{l}$  was reached. Reduction of disulfide bonds, alkylation, acetone precipitation, and digestion with trypsin were performed as described in recent works [4,5]. Labeling with TMT, C18 spin column purification, and high pH reversed-phase peptide fractionation into eight fractions were performed as described in a previous work [5].

**Liquid chromatography mass spectrometry:** The eight fractions containing the peptides were resuspended in 0.1% formic acid (FA) before liquid chromatography mass spectrometry was performed. Six microliters of each sample were injected into a Dionex RSLC nanoUPLC system connected to an Orbitrap Fusion mass spectrometer (Thermo Scientific, Waltham, MA) equipped with an Easy Spray ion source. Liquid chromatography and mass spectrometry in TMT synchronous precursor selection MS3 mode were performed as described in a previous work [4]. With the Sequest HT database, mass spectrometry raw data were searched against the Uniprot *Sus scrofa* database and the *Homo sapiens* Uniprot database using Proteome Discoverer 2.1 as previously described [5]. A false discovery rate of 1% was used to identify proteins. The false discovery rate was calculated using the automated false discovery rate calculations of Proteome Discoverer that uses a Decoy Database search to determine the false discovery rate.

**Statistical analysis:** Mass spectrometry data were further processed with Perseus (version 1.6.0.0) that was used to remove poorly identified proteins as described in a previous

article [4]. In Perseus, TMT abundances were log2 transformed, and a valid value in each of the ten samples was required. At least two unique peptides were required. A paired *t* test conducted in Perseus was used for statistical analysis. Before fold changes were calculated, the log2 transformation was reversed. Fold changes were then calculated as the ratio of TMT abundance of the right eye to the TMT abundance of the left eye. Proteins were considered statistically significantly changed if  $p < 0.05$  and fold change  $> 1.25$  or fold change  $< 0.8$ . Regulated keratins were considered contaminants.

**Western blotting:** Western blotting was conducted as previously described [4]. Samples for mass spectrometry were also used for western blotting after TEAB buffer was added. For this study, a primary monoclonal mouse anti- $\beta$ -actin antibody 1:5,000 (clone AC-15, Sigma-Aldrich, Søborg, Denmark) and a primary polyclonal sheep anti-transferrin (TTR) antibody 1:5,000 (ab9015, Abcam, Cambridge, UK) were used. Both antibodies were diluted in 2.5% (w/v) skim milk blocking buffer. Horseradish peroxidase (HRP)-conjugated secondary antibodies polyclonal goat anti-mouse immunoglobulins/HRP (Dako, Glostrup, Denmark) and rabbit anti-sheep IgG heavy and light chains (ab6747, Abcam, Cambridge, UK) were used, diluted 1:30,000 and 1:1,000, respectively, in 2.5% (w/v) skim milk blocking buffer.

**Immunohistochemistry:** Eyes from one animal were used for immunohistochemistry to compare BRVO + bevacizumab ( $n=1$ ) to BRVO + NaCl ( $n=1$ ). Immunohistochemical analyses were performed on retinal sections containing the occlusions. Fixation was performed using a fixative of 99% ethanol (three parts) and glacial acetic acid (one part) as previously described [4]. A polyclonal IgG antibody directed at TTR (ab9015, Abcam) was used for immunohistochemistry. Sheep antibodies were diluted (1:200 to 1:800) in PBS (1X; 137 mM NaCl, 2.7 mM KCl, 10 mM  $\text{Na}_2\text{HPO}_4$ , 1.8 mM  $\text{KH}_2\text{PO}_4$ , pH 7.4) with 0.3% Triton X100. Retinal sections were incubated overnight at 4 °C and were processed using EnVision (DakoCytomation, Glostrup, Denmark) DAB. Controls were incubated with either sheep IgG<sub>2b</sub> alone or irrelevant sheep antibodies.

## RESULTS

**Experimental branch retinal vein occlusion:** Experimental BRVO was successfully induced in both eyes of each animal based on the development of venous dilation and the appearance of flame-shaped hemorrhages (Figure 2). Fluorescein angiography 5 days after BRVO showed no recanalization of the occluded veins (Figure 3A,B).

**Protein quantification with mass spectrometry:** Results of the database search are provided in Appendix 1. A total of



Figure 2. Fundus image of BRVO obtained approximately 10 min after BRVO in the inferior retina. Branch retinal vein occlusion (BRVO) was considered successful when venous dilation and hemorrhages were observed upstream of the site of occlusion as seen in the image. Black arrow: site of occlusion.

TABLE 1. SIGNIFICANTLY CHANGED PROTEINS ORDERED ACCORDING TO FOLD CHANGE.				
UniProt ID	Protein name	Gene name	P-value	Fold change
P01834	Immunoglobulin kappa chain C region	IGKC	0.0039	12.50
P01857	Immunoglobulin gamma-1 chain C region	IGHG1	0.0054	11.55
P01860	Immunoglobulin gamma-3 chain C region	IGHG3	0.015	2.41
P50390	Transthyretin (TTR)	TTR	0.025	2.36
P04264	Keratin, type II cytoskeletal 1	KRT1	0.018	1.90
Q9H999	Pantothenate kinase 3	PANK3	0.014	1.31
O60245-2	Isoform B of Protocadherin-7	PCDH7	0.0016	0.79
Q9GZU8	Protein FAM192A	FAM192A	0.030	0.79
Q35914	ATP synthase protein 8	ATP8	0.011	0.76

4,013 proteins were successfully identified after filtering (Appendix 2). When no cut-offs were applied, 397 proteins were statistically significantly changed. When cut-offs were applied, a total of nine proteins were found to be statistically significantly changed following bevacizumab intervention (Table 1). Bepacizumab intervention resulted in upregulation of immunoglobulin kappa chain C region (fold change=12.50, p= 0.0039), immunoglobulin gamma-1 chain C region (fold change=11.55, p=0.0054), and immunoglobulin gamma-3 chain C region (fold change=2.41, p=0.015). Bepacizumab intervention also resulted in upregulation of TTR (fold

change=2.36, p=0.025) and pantothenate kinase 3 (fold change=1.31, p=0.014). A number of proteins were found to be statistically significantly downregulated. These proteins included isoform B of protocadherin 7 (fold change=0.79, p=0.0016), protein FAM192A (fold change=0.79, p=0.030), and ATP synthase protein 8 (fold change=0. 76, p=0.011).

*Immunohistochemistry and western blotting:* Immunohistochemistry revealed that TTR was present in all retinal layers and that TTR was abundant in the retinal vasculature regardless of bepacizumab intervention (Figure 4). Staining for TTR was particularly pronounced in the choroid in BRVO

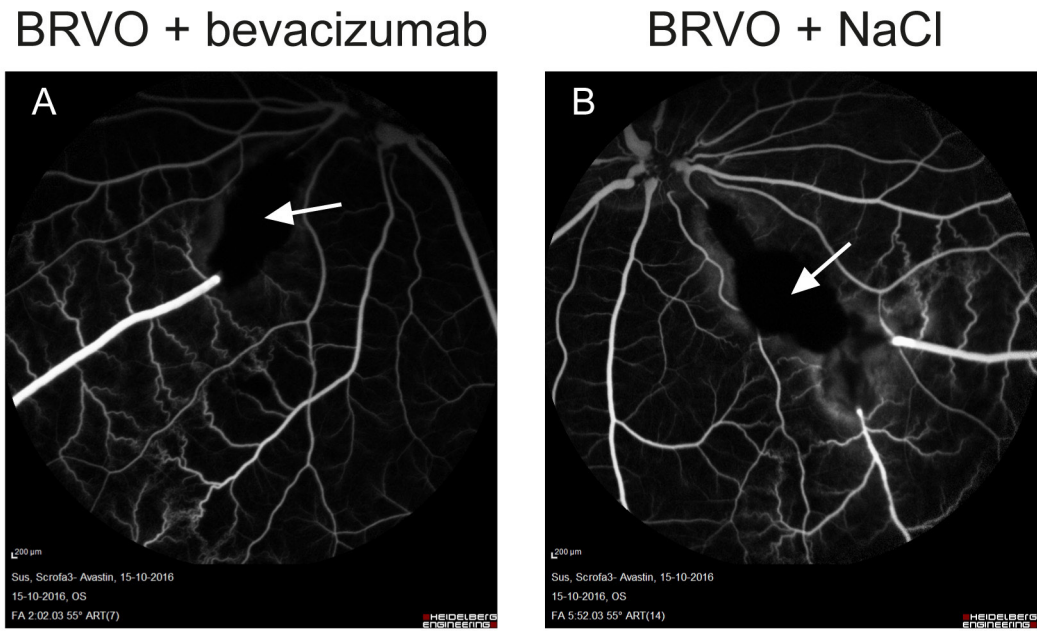


Figure 3. Fluorescein angiography was obtained 5 days after BRVO to confirm that no recanalization of the occluded veins had occurred. Images from the same animal are shown. No passage of fluorescein through the sites of occlusion is observed. **A:** Fluorescein angiography of branch retinal vein occlusion (BRVO) with bepacizumab intervention. White arrow: site of occlusion. **B:** Fluorescein angiography of BRVO without bepacizumab intervention. White arrow: site of occlusion.



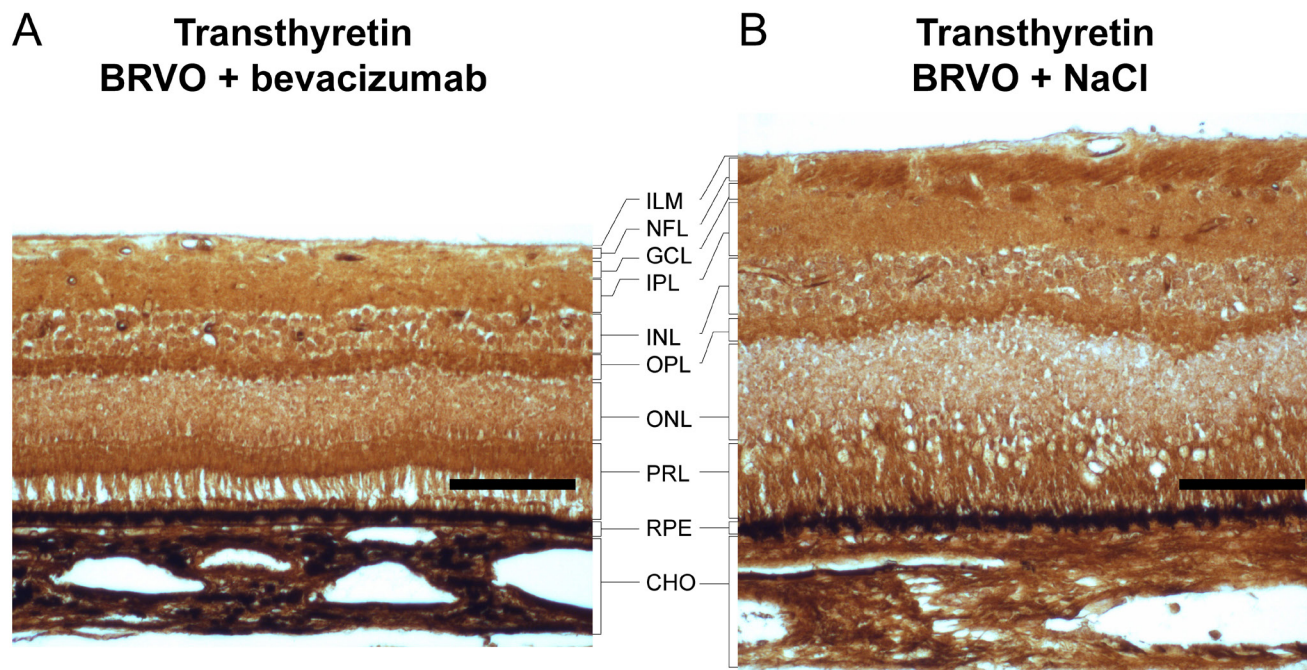


Figure 4. Immunohistochemical staining for TTR. Mass spectrometry revealed upregulation of transthyretin (TTR) which was further characterized with immunohistochemistry. Staining for TTR revealed that TTR was present in all retinal layers and in the choroid. A strong reaction for TTR was seen in the retinal vessels regardless of bevacizumab intervention. A: In branch retinal vein occlusion (BRVO) with bevacizumab intervention, a strong reaction for TTR was observed in the choroid. In the choroid, the reaction for TTR was stronger in BRVO with bevacizumab intervention (A) compared to BRVO without bevacizumab intervention (B). Therefore, the choroid may be the source of increased TTR in BRVO with bevacizumab intervention. Scale bar = 50  $\mu$ m. Reaction color: brown. Abbreviations: ILM: inner limiting membrane; NFL: nerve fiber layer; GCL: ganglion cell layer; IPL: inner plexiform layer; INL: inner nuclear layer; OPL: outer plexiform layer; ONL: outer nuclear layer; PRL: photoreceptor layer. RPE: retinal pigment epithelium. CHO: choroid.

treated with bevacizumab (Figure 4A) while choroid staining for TTR was weaker in BRVO treated with NaCl (Figure 4B). Western blotting confirmed the upregulation of TTR following bevacizumab intervention ( $p=0.045$ ; Figure 5).

## DISCUSSION

**Experimental BRVO and bevacizumab intervention:** Laser-induced BRVO is a well-established model, and we have shown in previous studies that occluded vessels do not recanalize [4-7]. In the present study, BRVO was validated with fluorescein angiography 5 days after BRVO. As we have previously demonstrated that occlusion is sustained in the model [4,7], we are confident that the vessels remained occluded throughout the study.

In the present study, the bevacizumab intervention was given shortly after BRVO was induced. From previous studies [5,7], we learned that some recovery takes place in experimental BRVO. Therefore, an intravitreal intervention should be given in the acute stage of BRVO [4]. Ideally, intravitreal

bevacizumab should be injected 24 h after experimental BRVO, but some animals may suffer from fatigue if they are exposed to anesthesia on 2 consecutive days. To give the intervention in the acute stage of BRVO and to avoid fatigue in the animals, the anti-VEGF intervention was administered approximately 15 min after BRVO.

**Focal adhesion and plasma proteins:** We previously demonstrated that BRVO results in upregulation of proteins involved in focal adhesion, including laminins, integrin  $\beta$ -1, osteopontin, talin-2, actinins, filamin-C, and myosin 9 [7]. The present study demonstrated that BRVO is associated with multiple protein changes that are not reversed through neutralization of VEGF with bevacizumab. Resistance to anti-VEGF treatment is a common phenomenon in the treatment of retinal vein occlusion [8], and some patients are considered anti-VEGF non-responders [9]. The fact that BRVO causes a multitude of protein alterations may explain why some patients do not respond to anti-VEGF therapy. Multiple protein changes in BRVO may also explain why

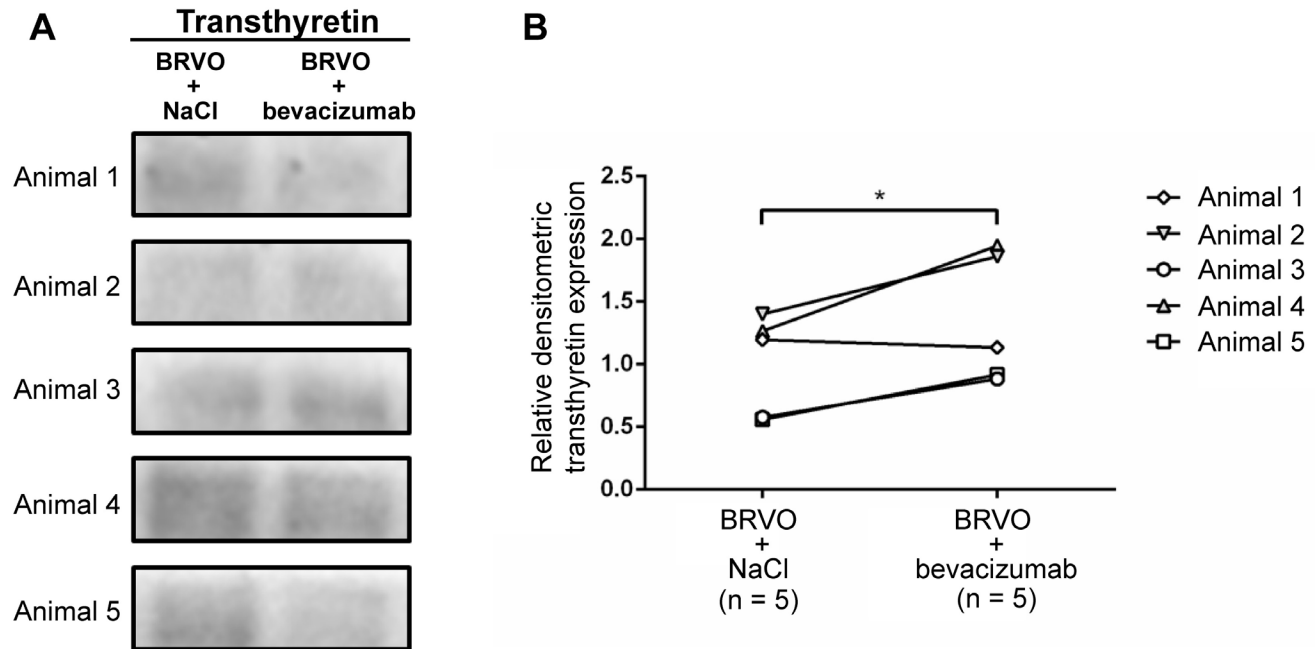


Figure 5. Western blot analysis of TTR. Western blotting confirmed that transthyretin (TTR) was statistically significantly increased in branch retinal vein occlusion (BRVO) treated with bevacizumab ( $p=0.045$ ). **A**: Retinal content of TTR. **B**: Densitometric change of relative TTR content between BRVO + NaCl and BRVO with bevacizumab intervention normalized to relative  $\beta$ -actin expression. \* $p<0.05$ .

visual function remains impaired despite successful treatment of macular edema and neutralization of VEGF.

BRVO is known to cause disruption of the blood–retinal barrier followed by an influx of plasma proteins, such as fibrinogen chains,  $\alpha$ -2-macroglobulin, and  $\beta$ -2-glycoprotein 1 [7]. Anti-VEGF treatments are known to reestablish the blood–retinal barrier and to diminish leakage of fluid and plasma proteins [3]. Therefore, a lower plasma protein content was likely to be observed in BRVO with bevacizumab intervention. However, there was no statistically significant difference in plasma proteins between BRVO with bevacizumab intervention and BRVO without bevacizumab intervention.

**Transthyretin:** Transthyretin is a tetramer consisting of four identical subunits. In the eye, TTR is synthesized by RPE cells but is known to have a wide distribution within the retinal layers [10,11]. TTR is a carrier of retinol binding protein and a minor carrier of thyroxine (T4) [12]. Immunohistochemistry revealed a reaction for TTR in all retinal layers, but a pronounced reaction for TTR was identified in the choroid following bevacizumab treatment. Thus, the choroid may be the source of the increased content of TTR measured in BRVO treated with bevacizumab.

We previously tested the anti-VEGF agent ranibizumab on the BRVO model. Interestingly, neutralization of VEGF-A with ranibizumab also resulted in an increased level of TTR

[5]. Thus, this is the second study in which we showed that anti-VEGF treatment increases retinal TTR in the BRVO model. Therefore, we find it highly unlikely that the increased level of TTR could be a result of multiple hypothesis testing. Although the data indicate that anti-VEGF agents increase the retinal content of TTR, the opposite scenario takes place in patients with mutations in the TTR gene who have been reported to have high levels of VEGF in the vitreous body. O’Hearn and coworkers [13] reported on a patient with an isolated Glu54Gly TTR mutation causing familial amyloidotic polyneuropathy. This patient had an elevated level of vitreous VEGF of 854 pg/ml while the VEGF level was 128 pg/ml in the vitreous from a control patient who underwent vitrectomy due to a macular hole. Zou et al. [14] reported on patients with the TTR Ala36Pro mutation which causes familial TTR amyloidosis. The vitreous VEGF concentration from patients with the TTR Ala36Pro mutation was found to be approximately threefold higher than in control patients with macular epiretinal membrane or macular hole. Furthermore, patients with the TTR Ala36Pro mutation had higher serum VEGF levels than healthy controls. Thus, case reports and our studies of the BRVO model suggest an interaction between TTR and VEGF, and we hypothesize that anti-VEGF agents exert a beneficial effect on the retina by upregulating TTR.

Mutations in the TTR gene are known to cause familial amyloidosis which often leads to ocular manifestations [15]. Patients with ocular manifestations generally have vitreous involvement with vitreous opacities [13-15]. Some patients with familial amyloidosis due to TTR mutations also present with tortuous retinal vessels, retinal hemorrhages, and neovascularization [13,15]. Veronese and coworkers [16] investigated the ocular manifestations of a patient with a rare amyloidogenic TTR Glu54Lys mutation. This patient was found to have sheathing of retinal vessels and retinal hemorrhages while fluorescein angiography showed microaneurysms and perivascular focal staining. Therefore, it may be considered whether TTR prevents development of neovascularizations and vascular leakage.

*Immunoglobulin heavy chains:* Bevacizumab intervention resulted in upregulation of three constant regions of immunoglobulin heavy chains. These chains included immunoglobulin kappa chain C region, immunoglobulin gamma-1 chain C region, and immunoglobulin gamma-3 chain C region. These immunoglobulin chains are likely to be components of bevacizumab. In experimental BRVO treated with the anti-VEGF agent ranibizumab, we previously identified increased levels of immunoglobulin kappa chain C region and immunoglobulin gamma-1 chain C region which are thought to be components of ranibizumab [5].

*Pantothenate kinase 3:* Pantothenate kinase 3 (PanK3) is one of the four mammalian pantothenate kinase isoforms that control the rate of coenzyme A (CoA) biosynthesis [17]. PanK3 catalyzes the first step of CoA biosynthesis. CoA is a cofactor in several reactions, such as oxidation of fatty acids, carbohydrates, and amino acids [18]. To the best of our knowledge, the role of retinal PanK3 remains largely unstudied.

*Protocadherin 7:* Protocadherin 7 is an integral membrane protein. Protocadherins play a key role in neuronal development [19]. Protocadherin 7 is known to be involved in cell proliferation, migration, and invasion [20]. Protocadherins are the largest cadherin subfamily [19]. The retinal distribution of protocadherin has been studied in ferret retinas as reported by Etzrodt and coworkers [19]. Protocadherin 7 is expressed in the nerve fiber layer, the ganglion cell layer, and the inner nuclear layer but is absent in the outer nuclear layer. The biological function of retinal protocadherin 7 remains largely unstudied.

*Anti-VEGF versus dexamethasone:* In the present study, we identified a total of nine proteins that were differentially regulated following bevacizumab intervention. This finding confirms that bevacizumab has a narrow mechanism of action in comparison to a dexamethasone (DEX) intravitreal

implant (OZURDEX, Allergan) that is an alternative to bevacizumab. We previously tested a DEX intravitreal implant on the experimental BRVO model [4]. Using the same criteria as in the present study, we identified 26 proteins that were statistically significantly changed following DEX intervention. Neutralization of VEGF-A with bevacizumab did not cause any changes in VEGF receptor-2 (VEGFR-2) in the BRVO model. In this aspect, bevacizumab differs from a DEX implant that causes a small downregulation of VEGFR-2 in experimental BRVO [4].

*Conclusions:* In experimental BRVO, bevacizumab increased the retinal level of TTR. Immunohistochemistry revealed pronounced staining for TTR in the choroid indicating that the choroid may be the source of TTR following bevacizumab intervention. This is the second study we have conducted that revealed an upregulation of TTR following anti-VEGF intervention in the BRVO model. We hypothesize that there is an interaction between TTR and VEGF and that anti-VEGF agents exert a beneficial effect on the retina by upregulating TTR. The proteomic analysis revealed that bevacizumab regulated only a limited number of retinal proteins and has a narrow mechanism of action compared to DEX intravitreal implants.

## APPENDIX 1.

To access the data, click or select the words “[Appendix 1.](#)”

## APPENDIX 2.

To access the data, click or select the words “[Appendix 2.](#)”

## ACKNOWLEDGMENTS

**Financial support:** The mass spectrometer used for the present study was kindly donated by A.P. Møller og Hustru Chastine Mc-Kinney Møllers Fond til almene Formaal. The study was funded by Fight for Sight Denmark, Svend Andersen Foundation, Bagger-Sørensen Foundation, Obel Family Foundation, Herta Christensen Foundation, the North Denmark Region (2013-0076797) and Speciallæge Heinrich Kopps Legat. **Disclosures:** Bevacizumab was purchased from the pharmacy of Aalborg University Hospital, Aalborg, Denmark. The authors have no financial interests to declare.

## REFERENCES

1. Rehak J, Rehak M. Branch retinal vein occlusion: pathogenesis, visual prognosis, and treatment modalities. *Curr Eye Res* 2008; 33:111-31. [PMID: 18293182].
2. Meyer CH, Holz FG. Preclinical aspects of anti-VEGF agents for the treatment of wet AMD: ranibizumab and



- bevacizumab. *Eye (Lond)* 2011; 25:661-72. [PMID: 21455242].
3. Cehofski LJ, Honore B, Vorum H. Review: Proteomics in Retinal Artery Occlusion, Retinal Vein Occlusion, Diabetic Retinopathy and Acquired Macular Disorders. *Int J Mol Sci* 2017; 18:909-[PMID: 28452939].
4. Cehofski LJ, Kruse A, Magnusdottir SO, Alsing AN, Kirkeby S, Honore B, Vorum H. Dexamethasone intravitreal implant downregulates PDGFR-alpha and upregulates caveolin-1 in experimental branch retinal vein occlusion. *Exp Eye Res* 2018; 171:174-82. [PMID: 29505751].
5. Cehofski LJ, Kruse A, Bogsted M, Magnusdottir SO, Stensballe A, Honore B, Vorum H. Retinal proteome changes following experimental branch retinal vein occlusion and intervention with ranibizumab. *Exp Eye Res* 2016; 152:49-56. [PMID: 27619476].
6. Cehofski LJ, Kruse A, Kjaergaard B, Stensballe A, Honore B, Vorum H. Dye Free Porcine Model of Experimental Branch Retinal Vein Occlusion – a Suitable Approach for Retinal Proteomics. *J Ophthalmol* 2015; 2015:839137-[PMID: 26064675].
7. Cehofski LJ, Kruse A, Kjaergaard B, Stensballe A, Honore B, Vorum H. Proteins involved in focal adhesion signaling pathways are differentially regulated in experimental branch retinal vein occlusion. *Exp Eye Res* 2015; 138:87-95. [PMID: 26086079].
8. Ashraf M, Souka AA, Singh RP. Central retinal vein occlusion: modifying current treatment protocols. *Eye (Lond)* 2016; 30:505-14. [PMID: 26869163].
9. Wolfe JD, Shah AR, Yonekawa Y, Al Faran A, Franklin MS, Abbey AM, Capone A Jr. Receiver operating characteristic curve to predict anti-VEGF resistance in retinal vein occlusions and efficacy of Ozurdex. *Eur J Ophthalmol* 2016; 26:168-73. [PMID: 26428221].
10. Dwork AJ, Cavallaro T, Martone RL, Goodman DS, Schon EA, Herbert J. Distribution of transthyretin in the rat eye. *Invest Ophthalmol Vis Sci* 1990; 31:489-96. [PMID: 2180844].
11. Cavallaro T, Martone RL, Dwork AJ, Schon EA, Herbert J. The retinal pigment epithelium is the unique site of transthyretin synthesis in the rat eye. *Invest Ophthalmol Vis Sci* 1990; 31:497-501. [PMID: 1690688].
12. Buxbaum JN, Roberts AJ, Adame A, Masliah E. Silencing of murine transthyretin and retinol binding protein genes has distinct and shared behavioral and neuropathologic effects. *Neuroscience* 2014; 275:352-64. [PMID: 24956283].
13. O'Hearn TM, Fawzi A, He S, Rao NA, Lim JI. Early onset vitreous amyloidosis in familial amyloidotic polyneuropathy with a transthyretin Glu54Gly mutation is associated with elevated vitreous VEGF. *Br J Ophthalmol* 2007; 91:1607-9. [PMID: 17522146].
14. Zou X, Dong F, Zhang S, Tian R, Sui R. Transthyretin Ala36Pro mutation in a Chinese pedigree of familial transthyretin amyloidosis with elevated vitreous and serum vascular endothelial growth factor. *Exp Eye Res* 2013; 110:44-9. [PMID: 23438977].
15. Reynolds MM, Veverka KK, Gertz MA, Dispenzieri A, Zeldenrust SR, Leung N, Pulido JS. Ocular Manifestations of Familial Transthyretin Amyloidosis. *Am J Ophthalmol* 2017; 183:156-62. [PMID: 28911993].
16. Veronese C, Marcheggiani EB, Tassi F, Gallelli I, Armstrong GW, Ciardella AP. Fundus autofluorescence imaging in hereditary ATTR amyloidosis with ocular involvement. *Amyloid* 2013; 20:269-71. [PMID: 23905621].
17. Leonardi R, Zhang YM, Yun MK, Zhou R, Zeng FY, Lin W, Cui J, Chen T, Rock CO, White SW, Jackowski S. Modulation of pantothenate kinase 3 activity by small molecules that interact with the substrate/allosteric regulatory domain. *Chem Biol* 2010; 17:892-902. [PMID: 20797618].
18. Zhang YM, Rock CO, Jackowski S. Feedback regulation of murine pantothenate kinase 3 by coenzyme A and coenzyme A thioesters. *J Biol Chem* 2005; 280:32594-601. [PMID: 16040613].
19. Etzrodt J, Krishna KK, Redies C. Expression of classic cadherins and delta-protocadherins in the developing ferret retina. *BMC Neurosci* 2009; 10:153-[PMID: 20028529].
20. Li AM, Tian AX, Zhang RX, Ge J, Sun X, Cao XC. Protocadherin-7 induces bone metastasis of breast cancer. *Biochem Biophys Res Commun* 2013; 436:486-90. [PMID: 23751349].

Articles are provided courtesy of Emory University and the Zhongshan Ophthalmic Center, Sun Yat-sen University, P.R. China. The print version of this article was created on 26 November 2018. This reflects all typographical corrections and errata to the article through that date. Details of any changes may be found in the online version of the article.